Classification of continuous phase transitions and stable phases. I. Six-dimensional order parameters

Jai Sam Kim, Dorian M. Hatch, and Harold T. Stokes
Department of Physics and Astronomy, Brigham Young University, Provo, Utah 84602
(Received 18 July 1985)

We have classified continuous phase transitions in physical systems where the order parameter transforms as a six-dimensional representation of a space group. The Landau potential is minimized with the use of Kim's geometrical method and a table of isotropy subgroups recently obtained by Stokes and Hatch. For most images of the active six-dimensional space-group representations, the complete list of stable phases is presented along with the corresponding region in coupling coefficient space (or pressure-temperature plane) for each stable phase.

I. INTRODUCTION

It is well known that Landau's phenomenological description[1] of a continuous phase transition is very useful in classifying symmetry changes which can take place during such a transition. A good illustrative example is given by Lyubarskii.[2] The procedure can be summarized as follows:

(1) Find the space group G of the high-symmetry phase of a physical system (crystal, alloy, etc.) and the irreducible representation ("irrep") Γ of the order parameter η responsible for the transition. The irrep should comply with the Landau and Lifshitz conditions[1,3] for a continuous commensurate phase transition (referred to as an active irrep[2]).

(2) Find a set of basic invariant polynomials in η up to degree four.

(3) Minimize the Landau potential consisting of this basic set of invariants and thus determine η_0 corresponding to the absolute minimum.

(4) Find the subgroup H of G that leaves fixed the order-parameter components η_0 at the absolute minimum found in step (3).

Step (3) is excessively laborious if carried out before step (4). Also, often one only needs to know the possible symmetries instead of the exact solution to (3). Birman[4] proposed that step (4) should be carried out before step (3) is attempted. If a subgroup H of the space group G is to be a symmetry group of the lower symmetry phase after a transition, the irrep Γ of G should subduce the identity representation of H at least once. (The number of times the identity representation occurs in the subduced representation is called the subduction frequency.) This is called the subduction criterion.[4] The group H is then called an "isotropy subgroup" of the representation Γ. The chain subduction criterion[5] further selects a minimal set of all "isotropy subgroups." If two "isotropy subgroups" H_1 and H_2 ($H_1 \supset H_2$) have the same subduction frequency, then H_2 is not eligible for any transition. That is, we need to consider only the largest "isotropy subgroup" in a chain of "isotropy subgroups" with the same subduction frequency. Normally there are many distinct chains at a given subduction frequency. The selection procedure needs to be carried out for all chains of "isotropy subgroups" at each subduction frequency,[6] starting from subduction frequency one down to the dimension of the order parameter. Good examples are given in Refs. 6 and 7. Since smaller "isotropy subgroups" do not appear in any physical context, the term isotropy subgroup is used in the literature for the largest "isotropy subgroup" in a given chain. The term maximal isotropy subgroup is used to label a member of the set of "high-level" isotropy subgroups of low index that are disjoint from each other and are supergroups of "lower level" ones of high index having higher subduction frequencies.

Many authors overlooked the direction of the order parameter that is left fixed by the elements of an isotropy subgroup (called the H-invariant vector of the isotropy subgroup). Vinberg *et al.*[8] made an extensive table, based on the above selection, of possible phase transitions in crystals with space group O_h^1 ($Pm3m$). In addition to listing isotropy subgroups, they included the invariant vector corresponding to each isotropy subgroup. The minimization procedure is greatly facilitated if the full information of the isotropy subgroups and their invariant vectors is available in advance.

In Kim's minimization method,[9] instead of working with order-parameter components, one treats each independent invariant polynomial as a variable. Furthermore the dependence of the potential on the radial and directional parts of η are separated. The directional minima of a low-degree Landau potential are obtained readily as a function of directions.[10] Then the absolute minimum is the lowest of all directional minima in the space of directions. The method utilizes already known geometrical properties of the orbit space.[11] An orbit[12] is the set of all representation vectors (order-parameter vectors in our case) that are connected by group elements. All vectors on an orbit yield the same numerical value for a group-invariant function and the isotropy subgroups leaving the vectors invariant are conjugate to each other. Thus a group-invariant function should be regarded as a function of the orbits rather than that of individual vectors. Conversely, an orbit can be completely specified by a set of l algebraically independent invariant polynomials. The number l is the dimension n of the representation vector

for finite groups, but is smaller than n for continuous compact groups. Without ambiguity we can call the space of the chosen l invariants the orbit space. Kim[9] has shown that the absolute minimum of a quartic invariant polynomial occurs at the boundary of the projected orbit space (with higher than quartic invariants discarded). It is known[11] that the boundary of the orbit space consists of orbits corresponding to "high-level" isotropy subgroups. Often the boundary of the projected orbit space is closed by orbits corresponding to first few "high-level" isotropy subgroups. In this case the information on the invariant vectors and isotropy subgroups is advantageous in building the orbit space (though one cannot tell it in advance). Once the orbit space is depicted, the phase diagram can be readily obtained.

The procedure of making a complete list of isotropy subgroups for an irrep of a space group can be carried out manually[6,7,13] using a table[14,15] of space-group representations. A systematic procedure for obtaining a complete list of isotropy subgroups has been given in the literature.[16,17] However, it is very laborious and thus mistake-prone. For point-group representations in three dimensions the list of isotropy subgroups has been tabulated in Ref. 18. For space-group representations the procedure is more complex and only some individual cases[2,6–8,19] have been analyzed. With the aid of a computer, Stokes and Hatch[20(a)] have made a complete list[20(b)] of isotropy subgroups of all subduction frequencies along with corresponding invariant vectors for all irreps (active or not) corresponding to points of symmetry in the Brillouin zone of each space group.

Such a complete list of isotropy subgroups can be quite useful, as explained below. First, in the application of Landau theory one normally imposes the Landau and Lifshitz conditions on the irreducible representation of the order parameter and truncates the free-energy expansion in order-parameter components to the fourth degree. The Ascher[21] and Michel-Radicati[22] conjectures state that a fourth-degree Landau potential (cubic terms possibly included) allows stable phases with maximal isotropy subgroups only. Some counterexamples[23,24] to the conjectures have recently been found. A phase with a submaximal isotropy subgroup is therefore also eligible as an equilibrium state. Second, attempts have been made to extend the applicability of the Landau theory to a certain class of first-order phase transitions.[25] A well-known example is the theory of $BaTiO_3$.[26] To explain discontinuous transitions in the framework of thermodynamic theory, one can ease the Landau and/or Lifshitz conditions or include higher-degree terms in the potential for active representations. A higher-degree potential allows[27,28] phases with "lower-level" isotropy subgroups as equilibria. If the potential is expanded to high enough degree, *all* isotropy subgroups can be realized. A good example is the cubic XY model.[29] (Often the fourth-degree potential cannot distinguish different phases. To lift the degeneracy one needs to consider higher-degree terms perturbatively.)

It was shown[30,18] that thousands of space-group irreps can be categorized into a much smaller number of images. The set of distinct matrices (image) of an n-dimensional irrep of a space group form an n-dimensional representation of a point group in n dimensions. With respect to appropriately chosen bases, the set of irreps with equivalent images yields the same basic set of invariants and thus the same thermodynamic potential. In addition, when the potential is truncated to the fourth degree, several images can yield the same potential. In this case the symmetry group of the potential is the centralizer, i.e., the maximal supergroup of the set of image groups that leaves the quartic potential invariant. Thus the classification of continuous phase transitions is further simplified and a compact table of possible second-order transitions for all active images can be constructed. Using this strategy, Tolédano and Tolédano[31] made an extensive list of active images and tabulated possible second-order phase transitions for each image. However, their table contains errors and is not complete. In order to make an error-free table we need to resort to computers and an efficient method of minimization.

In this paper we carry out this project using the isotropy-subgroup tables prepared by Stokes and Hatch[20(b)] using a computer and Kim's minimization technique.[8] We analyze in detail the Landau potentials of eight images for six-dimensional order parameters, classify the possible continuous phase transitions, and list the stable phases in each region of the phase space, i.e., coupling-coefficient space or the usual pressure-temperature (P-T) plane. (A similar program has been partially carried out by Tolédano and Meimarakis.[32]) These eight examples have some interesting features: (1) degeneracies that are lifted by higher-degree terms, (2) violation of the Ascher conjecture,[21] and (3) violation of the Michel-Radicati conjecture.[22]

II. IMAGES AND INTEGRITY BASIS

For six-dimensional irreducible representations of space groups, Gufan *et al.*[30] suggested that there can be, at most, six distinct images complying with the Lifshitz condition but not necessarily with the Landau condition. Tolédano and Tolédano[31] listed ten active images (labeled $L1$–$L10$). We have found an additional active image (we call it $L11$ to be consistent with the notation of Ref. 31).

The Landau potential can be expanded as a power series in the order parameters. Since it is a group-invariant polynomial series, it can be expressed as a polynomial series in a set (called the integrity basis) of basic invariant polynomials. We tabulate all six-dimensional active images along with the integrity basis up to the sixth degree in Table I. We use the international symbols[33] for space groups and those of Ref. 14 for representations. The basic invariant polynomials are listed in Table II.

III. ORBIT REPRESENTATIVES OF ACTIVE IMAGES

As we emphasized in the Introduction, knowledge of the orbit structure, and particularly the invariant vectors, is very useful in building the orbit space and thus in the analysis of a Landau potential. We use the method described in Ref. 17 to obtain the isotropy subgroups. Identification of the subgroups as one of the 230 space

TABLE I. Images of active six-dimensional space-group irreducible representations and their integrity bases up to the sixth degree. Irrep labeling is the same as in Ref. 14.

Image	Space-group irrep	Fourth-degree invariant	Sixth-degree invariant
$L1$	W_1, W_2, W_3, W_4 of O_h^5 ($Fm3m$; No. 225)	$I_1^{(4)}, I_2^{(4)}$	$I_1^{(6)}, I_2^{(6)}, I_3^{(6)}$
$L2$	W_1, W_2 of O^3 ($F432$; No. 209)	$I_1^{(4)}, I_2^{(4)}$	$I_1^{(6)}, I_2^{(6)}, I_3^{(6)}, I_4^{(6)}$
$L3$	W_1, W_2, W_3, W_4 of T_d^2 ($F\bar{4}3m$; No. 216)	$I_1^{(4)}, I_2^{(4)}$	$I_1^{(6)}, I_2^{(6)}, I_3^{(6)}$
$L4$	X_3, X_4 of $O_h^{(4)}$ ($Pn3m$; No. 224) $N_1^-, N_2^-, N_3^-, N_4^-$ of O_h^9 ($Im3m$; No. 229)	$I_1^{(4)}, I_2^{(4)}, I_3^{(4)}$	$I_1^{(6)}, I_2^{(6)}, I_3^{(6)}, I_5^{(6)}$
$L5$	N_2, N_4 of O^8 ($I4_132$; No. 214)	$I_1^{(4)}, I_2^{(4)}$	$I_1^{(6)}, I_2^{(6)}, I_3^{(6)}, I_6^{(6)}$
$L6$	N_2, N_4 of O^5 ($I432$; No. 211) N_2, N_3 of T_d^3 ($I\bar{4}3m$; No. 217) M_2 of O_h^2 ($Pn3n$; No. 222) M_4 of O_h^4 ($Pn3m$; No. 224) X_4 of O_h^7 ($Fd3m$; No. 227) X_4 of O_h^8 ($Fd3c$; No. 228) N_2^+, N_4^+ of O_h^9 ($Im3m$; No. 229)	$I_1^{(4)}, I_2^{(4)}, I_3^{(4)}$	$I_1^{(6)}, I_2^{(6)}, I_3^{(6)}, I_5^{(6)}$
$L7$	X_5 of T_d^1 ($P\bar{4}3m$; No. 215) X_5^+, X_5^-, M_5^- of O_h^1 ($Pm3m$; No. 221) M_5^- of O_h^3 ($Pm3n$; No. 223) X_5^- of O_h^5 ($Fm3m$; No. 225) X_5^- of O_h^6 ($Fm3c$; No. 226)	$I_1^{(4)}, I_2^{(4)}, I_3^{(4)}, I_6^{(4)}$	$I_1^{(6)}, I_2^{(6)}, I_3^{(6)}, I_5^{(6)}$ $I_7^{(6)}, I_8^{(6)}$
$L8$	N_1^-, N_2^- of T_h^5 ($Im3$; No. 204)	$I_1^{(4)}, I_2^{(4)}, I_3^{(4)}$	$I_1^{(6)}, I_2^{(6)}, I_3^{(6)}, I_5^{(6)}$ $I_9^{(6)}, I_{10}^{(6)}, I_{11}^{(6)}$
$L9$	X_3, X_4 of O_h^3 ($Pm3n$; No. 223)	$I_1^{(4)}, I_2^{(4)}, I_3^{(4)}, I_4^{(4)}$, $I_5^{(4)}$	$I_1^{(6)}, I_2^{(6)}$, $I_{12}^{(6)}, \ldots, I_{16}^{(6)}$
$L10$	$X_1 \oplus X_2$, $X_3 \oplus X_4$ of T_d^4 ($P\bar{4}3n$; No. 218)	$I_1^{(4)}, I_2^{(4)}, I_3^{()}, I_4^{(4)}$, $I_5^{(4)}, I_7^{(4)}, I_8^{(4)}, I_9^{(4)}$	$I_1^{(6)}, I_2^{(6)}$, $I_{12}^{(6)}, \ldots, I_{22}^{(6)}$
$L11$	$M_2 \oplus M_3$ of O^6 ($P4_332$; No. 212) $M_2 \oplus M_3$ of O^7 ($P4_132$; No. 213)	$I_1^{(4)}, I_2^{(4)}, I_7^{(4)}$	$I_1^{(6)}, I_2^{(6)}, I_3^{(6)}, I_4^{(6)}$, $I_6^{(6)}, I_{17}^{(6)}, I_{23}^{(6)}$

groups in a standard setting is discussed in Ref. 34. We follow that description here. An orbit representative is then obtained for each isotropy subgroup by usual group-theoretical projection techniques.[2] We tabulate the orbit representatives of all isotropy subgroups for each active image in Table III. (Our notation was dictated by ease of recognition: P stands for point, C for curve, and S for two-dimensional surface.) The corresponding isotropy subgroups which leave them invariant are different for each space group and representation. (See Ref. 35 for an example.) Thus they are not listed here, but will be listed elsewhere (Stokes and Hatch[20(b)]).

IV. IMAGES $L1$, $L2$, $L3$, AND $L5$

Let us consider the images $L1$, $L2$, $L3$, and $L5$, which yield the same fourth-degree Landau potential. Here our primary interest is in continuous phase transitions. We therefore will mainly be concerned with minimization of the fourth-degree potential. However, we shall see that it is necessary to keep the sixth-degree terms when degeneracies occur at the fourth degree.

The Landau free energy to the fourth degree is written

TABLE II. Basic invariant polynomials of the integrity bases for the images of Table I.

$$I_2=\eta_1^2+\zeta_1^2+\eta_2^2+\zeta_2^2+\eta_3^2+\zeta_3^2$$
$$I_1^{(4)}=\eta_1^4+\zeta_1^4+\eta_2^4+\zeta_2^4+\eta_3^4+\zeta_3^4$$
$$I_2^{(4)}=\eta_1^2\zeta_1^2+\eta_2^2\zeta_2^2+\eta_3^2\zeta_3^2$$
$$I_3^{(4)}=\eta_1\zeta_1\eta_2\zeta_2+\eta_2\zeta_2\eta_3\zeta_3+\eta_3\zeta_3\eta_1\zeta_1$$
$$I_4^{(4)}=\eta_1^2\eta_2^2+\zeta_1^2\zeta_2^2+\eta_2^2\eta_3^2+\zeta_2^2\zeta_3^2+\eta_3^2\eta_1^2+\zeta_3^2\zeta_1^2$$
$$I_5^{(4)}=\eta_1^2\zeta_2^2+\eta_2^2\zeta_3^2+\eta_3^2\zeta_1^2$$
$$I_6^{(4)}=\eta_1\zeta_1(\eta_2^2+\zeta_2^2-\eta_3^2-\zeta_3^2)+\eta_2\zeta_2(\eta_3^2+\zeta_3^2-\eta_1^2-\zeta_1^2)+\eta_3\zeta_3(\eta_1^2+\zeta_1^2-\eta_2^2-\zeta_2^2)$$
$$I_7^{(4)}=\eta_1\zeta_1(\eta_1^2-\zeta_1^2)+\eta_2\zeta_2(\eta_2^2-\zeta_2^2)+\eta_3\zeta_3(\eta_3^2-\zeta_3^2)$$
$$I_8^{(4)}=\eta_1\zeta_1(\eta_2^2-\zeta_3^2)+\eta_2\zeta_2(\eta_3^2-\zeta_1^2)+\eta_3\zeta_3(\eta_1^2-\zeta_2^2)$$
$$I_9^{(4)}=\eta_1\zeta_1(\zeta_2^2-\eta_3^2)+\eta_2\zeta_2(\zeta_3^2-\eta_1^2)+\eta_3\zeta_3(\zeta_1^2-\eta_2^2)$$
$$I_1^{(6)}=\eta_1^6+\zeta_1^6+\eta_2^6+\zeta_2^6+\eta_3^6+\zeta_3^6$$
$$I_2^{(6)}=\eta_1^2\zeta_1^2(\eta_1^2+\zeta_1^2)+\eta_2^2\zeta_2^2(\eta_2^2+\zeta_2^2)+\eta_3^2\zeta_3^2(\eta_3^2+\zeta_3^2)$$
$$I_3^{(6)}=(\eta_1^2-\zeta_1^2)(\eta_2^2-\zeta_2^2)(\eta_3^2-\zeta_3^2)$$
$$I_4^{(6)}=\eta_1\zeta_2\eta_2\zeta_2\eta_3\zeta_3$$
$$I_5^{(6)}=\eta_1\zeta_1\eta_2\zeta_2(\eta_3^2+\zeta_3^2)+\eta_2\zeta_2\eta_3\zeta_3(\eta_1^2+\zeta_1^2)+\eta_3\zeta_3\eta_1\zeta_1(\eta_2^2+\zeta_2^2)$$
$$I_6^{(6)}=\eta_1\zeta_1\eta_2\zeta_2(\eta_3^2-\zeta_3^2)+\eta_2\zeta_2\eta_3\zeta_3(\eta_1^2-\zeta_1^2)+\eta_3\zeta_3\eta_1\zeta_1(\eta_2^2-\zeta_2^2)$$
$$I_7^{(6)}=\eta_1\zeta_1\eta_2\zeta_2(\eta_1\zeta_1-\eta_2\zeta_2)+\eta_2\zeta_2\eta_3\zeta_3(\eta_2\zeta_2-\eta_3\zeta_3)+\eta_3\zeta_3\eta_1\zeta_1(\eta_3\zeta_3-\eta_1\zeta_1)$$
$$I_8^{(6)}=\eta_1\zeta_1(\eta_2^4+\zeta_2^4-\eta_3^4-\zeta_3^4)+\eta_2\zeta_2(\eta_3^4+\zeta_3^4-\eta_1^4-\zeta_1^4)+\eta_3\zeta_3(\eta_1^4+\zeta_1^4-\eta_2^4-\zeta_2^4)$$
$$I_9^{(6)}=(\eta_1^4+\zeta_1^4)(\eta_2^2+\zeta_2^2)+(\eta_2^4+\zeta_2^4)(\eta_3^2+\zeta_3^2)+(\eta_3^4+\zeta_3^4)(\eta_1^2+\zeta_1^2)$$
$$I_{10}^{(6)}=\eta_1^2\zeta_1^2(\eta_2^2+\zeta_2^2)+\eta_2^2\zeta_2^2(\eta_3^2+\zeta_3^2)+\eta_3^2\zeta_3^2(\eta_1^2+\zeta_1^2)$$
$$I_{11}^{(6)}=\eta_1\zeta_1\eta_2\zeta_2(\eta_1^2+\zeta_1^2)+\eta_2\zeta_2\eta_3\zeta_3(\eta_2^2+\zeta_2^2)+\eta_3\zeta_3\eta_1\zeta_1(\eta_3^2+\zeta_3^2)$$
$$I_{12}^{(6)}=\eta_1^2\eta_2^2\eta_3^2+\zeta_1^2\zeta_2^2\zeta_3^2$$
$$I_{13}^{(6)}=\eta_1^4\eta_2^2+\eta_2^4\eta_3^2+\eta_3^4\eta_1^2+\zeta_1^2\zeta_2^4+\zeta_2^2\zeta_3^4+\zeta_3^2\zeta_1^4$$
$$I_{14}^{(6)}=\eta_1^4\zeta_2^2+\eta_2^4\zeta_3^2+\eta_3^4\zeta_1^2+\eta_1^2\zeta_2^4+\eta_2^2\zeta_3^4+\eta_3^2\zeta_1^4$$
$$I_{15}^{(6)}=\eta_1\zeta_1\eta_2\zeta_2(\eta_1^2+\zeta_2^2)+\eta_2\zeta_2\eta_3\zeta_3(\eta_2^2+\zeta_3^2)+\eta_3\zeta_3\eta_1\zeta_1(\eta_3^2+\zeta_1^2)$$
$$I_{16}^{(6)}=\eta_1\zeta_1\eta_2\zeta_2(\zeta_1^2+\eta_2^2)+\eta_2\zeta_2\eta_3\zeta_3(\zeta_2^2+\eta_3^2)+\eta_3\zeta_3\eta_1\zeta_1(\zeta_3^2+\eta_1^2)$$
$$I_{17}^{(6)}=\eta_1\zeta_1(\eta_1^4-\zeta_1^4)+\eta_2\zeta_2(\eta_2^4-\zeta_2^4)+\eta_3\zeta_3(\eta_3^4-\zeta_3^4)$$
$$I_{18}^{(6)}=\eta_1\zeta_1(\eta_2^4-\zeta_3^4)+\eta_2\zeta_2(\eta_3^4-\zeta_1^4)+\eta_3\zeta_3(\eta_1^4-\zeta_2^4)$$
$$I_{19}^{(6)}=\eta_1\zeta_1(\eta_3^4-\zeta_2^4)+\eta_2\zeta_2(\eta_1^4-\zeta_3^4)+\eta_3\zeta_3(\eta_2^4-\zeta_1^4)$$
$$I_{20}^{(6)}=\eta_1\zeta_1(\eta_1^2\eta_2^2-\zeta_3^2\zeta_1^2)+\eta_2\zeta_2(\eta_2^2\eta_3^2-\zeta_1^2\zeta_2^2)+\eta_3\zeta_3(\eta_3^2\eta_1^2-\zeta_2^2\zeta_3^2)$$
$$I_{21}^{(6)}=\eta_1\zeta_1(\eta_1^2\eta_3^2-\zeta_2^2\zeta_1^2)+\eta_2\zeta_2(\eta_2^2\eta_1^2-\zeta_3^2\zeta_2^2)+\eta_3\zeta_3(\eta_3^2\eta_2^2-\zeta_1^2\zeta_3^2)$$
$$I_{22}^{(6)}=\eta_1\zeta_1(\eta_1^2\zeta_2^2-\eta_3^2\zeta_1^2)+\eta_2\zeta_2(\eta_2^2\zeta_3^2-\eta_1^2\zeta_2^2)+\eta_3\zeta_3(\eta_3^2\zeta_1^2-\eta_2^2\zeta_3^2)$$
$$I_{23}^{(6)}=\eta_1\zeta_1(\eta_2^2-\zeta_2^2)(\eta_3^2-\zeta_3^2)+\eta_2\zeta_2(\eta_3^2-\zeta_3^2)(\eta_1^2-\zeta_1^2)+\eta_3\zeta_3(\eta_1^2-\zeta_1^2)(\eta_2^2-\zeta_2^2)$$

$$G=\frac{a}{2}I_2+\tfrac{1}{4}(A_0I_2^2+A_1I_1^{(4)}+A_2I_2^{(4)})$$
$$\equiv\frac{a}{2}\eta^2+\tfrac{1}{4}\eta^4(A_0+A_1\lambda_1+A_2\lambda_2)\,, \tag{1}$$

with $\eta^2\equiv I_2$, $\lambda_1\equiv I_1^{(4)}/I_2^2$, and $\lambda_2\equiv I_2^{(4)}/I_2^2$. As usual, the positivity condition $A_0+A_1\lambda_1+A_2\lambda_2>0$ is assumed. The coefficients a, A_0, A_1, and A_2 carry the pressure and temperature dependence of the free energy. The radial and directional behaviors of the potential have been separated. The directional minimum[9] along a direction specified by λ_1 and λ_2 is given by

$$\eta_0^2=-\frac{a}{A_0+A_1\lambda_1+A_2\lambda_2}\,, \tag{2}$$

$$G_0(\lambda_1,\lambda_2)=-\frac{1}{4}\frac{a^2}{A_0+A_1\lambda_1+A_2\lambda_2}\,. \tag{3}$$

An arbitrary point (λ_1,λ_2) evaluated for any order-parameter components η_i lies within the shaded region in Fig. 1, which was, somewhat ambiguously but not misleadingly, called the "orbit space."[36]

The absolute minimum is found[9] by letting the contour equation (3) meet the "orbit space" starting from $G_0=-\infty$. At given temperature and pressure the contour is a straight line in the (λ_1,λ_2) plane with a fixed slope. The absolute minimum is found at the "orbit-space" boundary point where the line makes the first contact. In other words, one needs to find the extreme boundary point of the "orbit space" for given A_1 and A_2. One can immediately notice that at fourth degree only the protrudent orbits, $P1$, $P2$, $(P6,P7)$, and $(P11,P12)$, can yield the absolute minimum.

The stable phases can be readily classified as illustrated in the following. The reader will find Table IV useful for this purpose. In the region $A_1>0$, $A_2>0$, the line given by Eq. (3) has a negative slope and moves in the upper-right direction as G_0 increases. We see from Fig. 1 that four phases, $(P6,P7)$ and $(P11,P12)$, are eligible for the absolute minimum and are thus eligible as continuous transitions. The phases $(P6,P7)$ are stable in the subregion

$$G_0(P6)=G_0(\lambda_1=\tfrac{1}{3},\lambda_2=0)$$
$$<G_0(P11)=G_0(\lambda_1=\tfrac{1}{6},\lambda_2=\tfrac{1}{12})$$

or

$$2A_1-A_2<0\,.$$

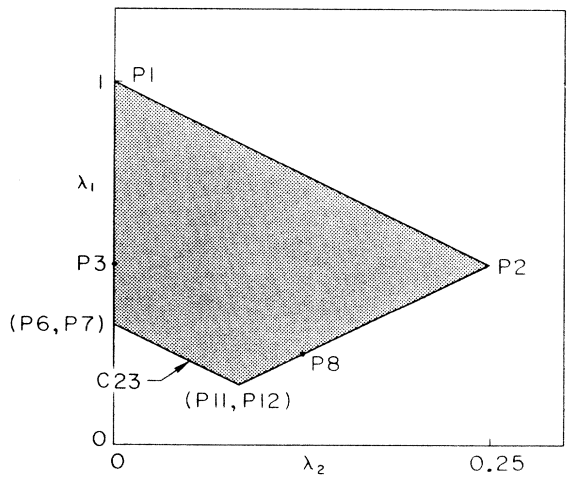

FIG. 1. The "orbit space" (λ_1,λ_2) of images $L1$, $L2$, $L3$, and $L5$.

TABLE III. Orbit structure of each six-dimensional image. An orbit of maximal isotropy subgroup is marked with an asterisk. Dim is the dimension of the orbit or the subduction frequency.

Label	Dim	Invariant vector	Label	Dim	Invariant vector
		Image $L1$			
$P1^*$	1	$a\ 0\ 0\ 0\ 0\ 0$	$S1$	3	$a\ b\ c\ 0\ 0\ 0$
$P2^*$	1	$a\ a\ 0\ 0\ 0\ 0$	$S3$	3	$a\ 0\ b\ 0\ c\ 0$
$P3^*$	1	$a\ 0\ a\ 0\ 0\ 0$	$S4$	3	$0\ a\ 0\ b\ 0\ c$
$P6^*$	1	$a\ 0\ a\ 0\ a\ 0$	$S6$	3	$a\ a\ b\ c\ 0\ 0$
$P7^*$	1	$0\ a\ 0\ a\ 0\ a$	$S8$	3	$a\ 0\ a\ 0\ b\ c$
$P8^*$	1	$a\ a\ a\ a\ 0\ 0$	$S9$	3	$a\ a\ b\ b\ c\ 0$
$P11^*$	1	$a\ a\ a\ a\ a\ a$	$S10$	3	$a\ b\ a\ b\ c\ 0$
			$S11$	3	$a\ b\ a\ b\ 0\ c$
$C1$	2	$a\ b\ 0\ 0\ 0\ 0$	$S14$	3	$a\ a\ a\ a\ b\ c$
$C2$	2	$a\ 0\ b\ 0\ 0\ 0$	$S15$	3	$a\ a\ b\ b\ c\ c$
$C5$	2	$a\ a\ b\ 0\ 0\ 0$			
$C8$	2	$a\ 0\ a\ 0\ b\ 0$	$4D1$	4	$a\ b\ c\ d\ 0\ 0$
$C9$	2	$0\ a\ 0\ a\ 0\ b$	$4D2$	4	$a\ b\ c\ 0\ d\ 0$
$C11$	2	$a\ a\ b\ b\ 0\ 0$	$4D3$	4	$a\ a\ b\ b\ c\ d$
$C14$	2	$a\ b\ a\ b\ 0\ 0$	$4D6$	4	$a\ b\ a\ b\ c\ d$
$C18$	2	$a\ a\ a\ a\ b\ 0$	$5D1$	5	$a\ b\ c\ d\ e\ 0$
$C21$	2	$a\ a\ a\ a\ b\ b$	$6D1$	6	$a\ b\ c\ d\ e\ f$
$C23$	2	$a\ b\ a\ b\ a\ b$			
		Image $L2$			
$P1^*$	1	$a\ 0\ 0\ 0\ 0\ 0$	$C22$	2	$a\ a\ a\ a\ b\ -b$
$P2^*$	1	$a\ a\ 0\ 0\ 0\ 0$	$C23$	2	$a\ b\ a\ b\ a\ b$
$P3^*$	1	$a\ 0\ a\ 0\ 0\ 0$			
$P6^*$	1	$a\ 0\ a\ 0\ a\ 0$	$S1$	3	$a\ b\ c\ 0\ 0\ 0$
$P7^*$	1	$0\ a\ 0\ a\ 0\ a$	$S3$	3	$a\ 0\ b\ 0\ c\ 0$
$P8^*$	1	$a\ a\ a\ a\ 0\ 0$	$S4$	3	$0\ a\ 0\ b\ 0\ c$
$P11^*$	1	$a\ a\ a\ a\ a\ a$	$S6$	3	$a\ a\ b\ c\ 0\ 0$
$P12^*$	1	$a\ a\ a\ a\ a\ -a$	$S8$	3	$a\ 0\ a\ 0\ b\ c$
			$S14$	3	$a\ a\ a\ a\ b\ c$
$C1$	2	$a\ b\ 0\ 0\ 0\ 0$	$S15$	3	$a\ a\ b\ b\ c\ c$
$C2$	2	$a\ 0\ b\ 0\ 0\ 0$	$S16$	3	$a\ a\ b\ b\ c\ -c$
$C5$	2	$a\ a\ b\ 0\ 0\ 0$			
$C8$	2	$a\ 0\ a\ 0\ b\ 0$	$4D1$	4	$a\ b\ c\ d\ 0\ 0$
$C9$	2	$0\ a\ 0\ a\ 0\ b$	$4D2$	4	$a\ b\ c\ 0\ d\ 0$
$C11$	2	$a\ a\ b\ b\ 0\ 0$	$4D3$	4	$a\ a\ b\ b\ c\ d$
$C14$	2	$a\ b\ a\ b\ 0\ 0$	$4D6$	4	$a\ b\ a\ b\ c\ d$
$C21$	2	$a\ a\ a\ a\ b\ b$	$6D1$	6	$a\ b\ c\ d\ e\ f$
		Image $L3$			
$P1^*$	1	$a\ 0\ 0\ 0\ 0\ 0$	$C18$	2	$a\ a\ a\ a\ b\ 0$
$P2^*$	1	$a\ a\ 0\ 0\ 0\ 0$	$C23$	2	$a\ b\ a\ b\ a\ b$
$P3^*$	1	$a\ 0\ a\ 0\ 0\ 0$			
$P6^*$	1	$a\ 0\ a\ 0\ a\ 0$	$S1$	3	$a\ b\ c\ 0\ 0\ 0$
$P7^*$	1	$0\ a\ 0\ a\ 0\ a$	$S3$	3	$a\ 0\ b\ 0\ c\ 0$
$P8^*$	1	$a\ a\ a\ a\ 0\ 0$	$S4$	3	$0\ a\ 0\ b\ 0\ c$
$P11^*$	1	$a\ a\ a\ a\ a\ a$	$S6$	3	$a\ a\ b\ c\ 0\ 0$
			$S8$	3	$a\ 0\ a\ 0\ b\ c$
$C1$	2	$a\ b\ 0\ 0\ 0\ 0$	$S10$	3	$a\ b\ a\ b\ c\ 0$
$C2$	2	$a\ 0\ b\ 0\ 0\ 0$	$S11$	3	$a\ b\ a\ b\ 0\ c$
$C5$	2	$a\ a\ b\ 0\ 0\ 0$	$S15$	3	$a\ a\ b\ b\ c\ c$
$C8$	2	$a\ 0\ a\ 0\ b\ 0$	$4D1$	4	$a\ b\ c\ d\ 0\ 0$
$C9$	2	$0\ a\ 0\ a\ 0\ b$	$4D2$	4	$a\ b\ c\ 0\ d\ 0$
$C11$	2	$a\ a\ b\ b\ 0\ 0$	$4D3$	4	$a\ a\ b\ b\ c\ d$
$C14$	2	$a\ b\ a\ b\ 0\ 0$	$6D1$	6	$a\ b\ c\ d\ e\ f$

TABLE III. (*Continued*).

Label	Dim	Invariant vector	Label	Dim	Invariant vector
		Image $L4$			
$P1^*$	1	$a\ 0\ 0\ 0\ 0\ 0$	$C21$	2	$a\ a\ a\ a\ b\ b$
$P2^*$	1	$a\ a\ 0\ 0\ 0\ 0$	$C22$	2	$a\ a\ a\ a\ b\ -b$
$P3^*$	1	$a\ 0\ a\ 0\ 0\ 0$	$C23$	2	$a\ b\ a\ b\ a\ b$
$P6^*$	1	$a\ 0\ a\ 0\ a\ 0$			
$P7^*$	1	$0\ a\ 0\ a\ 0\ a$	$S3$	3	$a\ 0\ b\ 0\ c\ 0$
$P8^*$	1	$a\ a\ a\ a\ 0\ 0$	$S4$	3	$0\ a\ 0\ b\ 0\ c$
$P9^*$	1	$a\ a\ a\ -a\ 0\ 0$	$S6$	3	$a\ a\ b\ c\ 0\ 0$
$P11^*$	1	$a\ a\ a\ a\ a\ a$	$S12$	3	$a\ b\ a\ -b\ c\ 0$
			$S13$	3	$a\ b\ a\ -b\ 0\ c$
$C1$	2	$a\ b\ 0\ 0\ 0\ 0$	$S14$	3	$a\ a\ a\ a\ b\ c$
$C2$	2	$a\ 0\ b\ 0\ 0\ 0$	$S15$	3	$a\ a\ b\ b\ c\ c$
$C8$	2	$a\ 0\ a\ 0\ b\ 0$	$S16$	3	$a\ a\ b\ b\ c\ -c$
$C9$	2	$0\ a\ 0\ a\ 0\ b$			
$C11$	2	$a\ a\ b\ b\ 0\ 0$	$4D1$	4	$a\ b\ c\ d\ 0\ 0$
$C12$	2	$a\ a\ b\ -b\ 0\ 0$	$4D3$	4	$a\ a\ b\ b\ c\ d$
$C14$	2	$a\ b\ a\ b\ 0\ 0$	$4D4$	4	$a\ a\ b\ c\ d\ -d$
$C15$	2	$a\ b\ a\ -b\ 0\ 0$	$4D6$	4	$a\ b\ a\ b\ c\ d$
$C19$	2	$a\ a\ a\ -a\ b\ 0$	$6D1$	6	$a\ b\ c\ d\ e\ f$
		Image $L5$			Image $L6$
$P1^*$	1	$a\ 0\ 0\ 0\ 0\ 0$	$P1^*$	1	$a\ 0\ 0\ 0\ 0\ 0$
$P2^*$	1	$a\ a\ 0\ 0\ 0\ 0$	$P2^*$	1	$a\ a\ 0\ 0\ 0\ 0$
$P3^*$	1	$a\ 0\ a\ 0\ 0\ 0$	$P3^*$	1	$a\ 0\ a\ 0\ 0\ 0$
$P6^*$	1	$a\ 0\ a\ 0\ a\ 0$	$P6^*$	1	$a\ 0\ a\ 0\ a\ 0$
$P7^*$	1	$0\ a\ 0\ a\ 0\ a$	$P7^*$	1	$0\ a\ 0\ a\ 0\ a$
$P8^*$	1	$a\ a\ a\ a\ 0\ 0$	$P8^*$	1	$a\ a\ a\ a\ 0\ 0$
			$P9^*$	1	$a\ a\ a\ -a\ 0\ 0$
$C1$	2	$a\ b\ 0\ 0\ 0\ 0$	$P11^*$	1	$a\ a\ a\ a\ a\ a$
$C14$	2	$a\ b\ a\ b\ 0\ 0$			
$C23$	2	$a\ b\ a\ b\ a\ b$	$C1$	2	$a\ b\ 0\ 0\ 0\ 0$
			$C12$	2	$a\ a\ b\ -b\ 0\ 0$
$S4$	3	$0\ a\ 0\ b\ 0\ c$	$C14$	2	$a\ b\ a\ b\ 0\ 0$
$S9$	3	$a\ a\ b\ b\ c\ 0$	$C22$	2	$a\ a\ a\ a\ b\ -b$
$S12$	3	$a\ b\ a\ -b\ c\ 0$	$C23$	2	$a\ b\ a\ b\ a\ b$
$6D1$	6	$a\ b\ c\ d\ e\ f$	$S4$	3	$0\ a\ 0\ b\ 0\ c$
			$S12$	3	$a\ b\ a\ -b\ c\ 0$
			$S15$	3	$a\ a\ b\ b\ c\ c$
			$4D3$	4	$a\ a\ b\ b\ c\ d$
			$6D1$	6	$a\ b\ c\ d\ e\ f$
		Image $L7$			
$P1^*$	1	$a\ 0\ 0\ 0\ 0\ 0$	$C20$	2	$a\ a\ b\ 0\ a\ -a$
$P2^*$	1	$a\ a\ 0\ 0\ 0\ 0$	$C23$	2	$a\ b\ a\ b\ a\ b$
$P6^*$	1	$a\ 0\ a\ 0\ a\ 0$			
$P7^*$	1	$0\ a\ 0\ a\ 0\ a$	$S6$	3	$a\ a\ b\ c\ 0\ 0$
$P9^*$	1	$a\ a\ a\ -a\ 0\ 0$	$S7$	3	$a\ a\ 0\ 0\ b\ c$
$P10^*$	1	$a\ a\ 0\ 0\ a\ -a$	$S12$	3	$a\ b\ a\ -b\ c\ 0$
$P11^*$	1	$a\ a\ a\ a\ a\ a$	$S13$	3	$a\ b\ a\ -b\ 0\ c$
			$S15$	3	$a\ a\ b\ b\ c\ c$
$C1$	2	$a\ b\ 0\ 0\ 0\ 0$	$S16$	3	$a\ a\ b\ b\ c\ -c$
$C11$	2	$a\ a\ b\ b\ 0\ 0$			
$C12$	2	$a\ a\ b\ -b\ 0\ 0$	$4D1$	4	$a\ b\ c\ d\ 0\ 0$
$C13$	2	$a\ a\ 0\ 0\ b\ -b$	$4D3$	4	$a\ a\ b\ b\ c\ d$
$C15$	2	$a\ b\ a\ -b\ 0\ 0$	$4D4$	4	$a\ a\ b\ c\ d\ -d$
$C19$	2	$a\ a\ a\ -a\ b\ 0$	$4D5$	4	$a\ a\ b\ -b\ c\ d$
			$6D1$	6	$a\ b\ c\ d\ e\ f$

TABLE III. (*Continued*).

Label	Dim	Invariant vector	Label	Dim	Invariant vector
		Image $L8$			Image $L9$
$P1^*$	1	$a\ 0\ 0\ 0\ 0\ 0$	$P1^*$	1	$a\ 0\ 0\ 0\ 0\ 0$
$P2^*$	1	$a\ a\ 0\ 0\ 0\ 0$	$P2^*$	1	$a\ a\ 0\ 0\ 0\ 0$
$P6^*$	1	$a\ 0\ a\ 0\ a\ 0$	$P4^*$	1	$a\ 0\ 0\ a\ 0\ 0$
$P7^*$	1	$0\ a\ 0\ a\ 0\ a$	$P5^*$	1	$0\ a\ a\ 0\ 0\ 0$
$P11^*$	1	$a\ a\ a\ a\ a\ a$	$P6^*$	1	$a\ 0\ a\ 0\ a\ 0$
			$P11^*$	1	$a\ a\ a\ a\ a\ a$
$C1$	2	$a\ b\ 0\ 0\ 0\ 0$			
$C2$	2	$a\ 0\ b\ 0\ 0\ 0$	$C1$	2	$a\ b\ 0\ 0\ 0\ 0$
$C11$	2	$a\ a\ b\ b\ 0\ 0$	$C2$	2	$a\ 0\ b\ 0\ 0\ 0$
$C12$	2	$a\ a\ b\ -b\ 0\ 0$	$C3$	2	$a\ 0\ 0\ b\ 0\ 0$
$C23$	2	$a\ b\ a\ b\ a\ b$	$C4$	2	$0\ a\ b\ 0\ 0\ 0$
			$C16$	2	$a\ b\ b\ a\ 0\ 0$
$S3$	3	$a\ 0\ b\ 0\ c\ 0$	$C17$	2	$a\ b\ -b\ a\ 0\ 0$
$S4$	3	$0\ a\ 0\ b\ 0\ c$	$C23$	2	$a\ b\ a\ b\ a\ b$
$S6$	3	$a\ a\ b\ c\ 0\ 0$			
$S7$	3	$a\ a\ 0\ 0\ b\ c$	$S3$	3	$a\ 0\ b\ 0\ c\ 0$
$S15$	3	$a\ a\ b\ b\ c\ c$	$S5$	3	$a\ 0\ b\ 0\ 0\ c$
$S16$	3	$a\ a\ b\ b\ c\ -c$	$S18$	3	$a\ a\ b\ c\ c\ b$
$4D1$	4	$a\ b\ c\ d\ 0\ 0$	$4D1$	4	$a\ b\ c\ d\ 0\ 0$
$4D3$	4	$a\ a\ b\ b\ c\ d$	$6D1$	6	$a\ b\ c\ d\ e\ f$
$4D4$	4	$a\ a\ b\ c\ d\ -d$			
$6D1$	6	$a\ b\ c\ d\ e\ f$			
		Image $L10$			Image $L11$
$C1^*$	2	$a\ b\ 0\ 0\ 0\ 0$	$C1^*$	2	$a\ b\ 0\ 0\ 0\ 0$
$C17^*$	2	$a\ b\ -b\ a\ 0\ 0$	$C14^*$	2	$a\ b\ a\ b\ 0\ 0$
$C23^*$	2	$a\ b\ a\ b\ a\ b$	$C23^*$	2	$a\ b\ a\ b\ a\ b$
$4D1$	4	$a\ b\ c\ d\ 0\ 0$	$6D1$	6	$a\ b\ c\ d\ e\ f$
$6D1$	6	$a\ b\ c\ d\ e\ f$			

We similarly obtain the stable phases in each region of the (A_1,A_2) space and give them in Table V.

The orbit points $P3$ and $P8$ are not protrudent, so they cannot yield the absolute minimum of the fourth-degree potential. Higher-degree expansions will make them eligible,[27,28] however. Also, the degeneracies between pairs of inequivalent orbits can be lifted by higher-degree terms. The degeneracy between $P6$ and $P7$ is lifted by $I_3^{(6)}$.

A. Images $L1$ and $L3$

Images $L1$ and $L3$ have the identical integrity basis up to the tenth degree. Twelfth-degree terms are needed to distinguish these two images. The direction $P11$ can be turned onto the direction $P12$ by a group rotation belonging to $L1$ or $L3$. Thus $P11$ and $P12$ correspond to different domains or equivalent isotropy subgroups, i.e., they are members of the same orbit.

B. Image $L2$

$P11$ and $P12$ cannot be connected by any group transformation belonging to $L2$. The degeneracy between them is lifted by $I_4^{(6)}$.

C. Image $L5$

The symmetry group of the physical system, image $L5$, is a subgroup of the symmetry group of the quartic potential, image $L1$. ($P11$,$P12$) are special points on the orbit $C23$ ($a=b$) of a submaximal isotropy subgroup in the case of $L5$ (whereas their isotropy subgroup was maximal in the case of $L1$). Stability of the orbit point $P11$ therefore violates the Ascher conjecture.[21] A counterexample to the Ascher conjecture in a four-dimensional case was previously discussed by Tolédano and Tolédano.[23]

Before we leave this section we would like to make a few comments relevant to all of the above. As the temperature is lowered through some critical temperature, the coefficient a becomes negative and a continuous phase transition takes place. Since the parameters (A_0,A_1,A_2) change with temperature and pressure, it may happen that the contour equation (3) becomes parallel to one of the boundary lines in the region $a<0$. At first glance it seems that a phase transition between the two adjacent low-symmetry phases (e.g., $P6$ and $P11$) jointed by a line may occur by continuous changes in η through an intermediate phase (the line). Since the individual order-

TABLE IV. Orbits of maximal isotropy subgroups and orbit parameters λ_i's.

Phases	Invariant vector	λ_1	λ_2	λ_3	λ_7
$P1$	$a\ 0\ 0\ 0\ 0\ 0$	1	0	0	0
$P2$	$a\ a\ 0\ 0\ 0\ 0$	$\frac{1}{2}$	$\frac{1}{4}$	0	0
$P3$	$a\ 0\ a\ 0\ 0\ 0$	$\frac{1}{2}$	0	0	0
$P4$	$a\ 0\ 0\ a\ 0\ 0$	$\frac{1}{2}$	0	0	0
$P5$	$0\ a\ a\ 0\ 0\ 0$	$\frac{1}{2}$	0	0	0
$P6$	$a\ 0\ a\ 0\ a\ 0$	$\frac{1}{3}$	0	0	0
$P7$	$0\ a\ 0\ a\ 0\ a$	$\frac{1}{3}$	0	0	0
$P8$	$a\ a\ a\ a\ 0\ 0$	$\frac{1}{4}$	$\frac{1}{8}$	$\frac{1}{16}$	0
$P9$	$a\ a\ a\ -a\ 0\ 0$	$\frac{1}{4}$	$\frac{1}{8}$	$-\frac{1}{16}$	0
$P10$	$a\ a\ 0\ 0\ a\ -a$	$\frac{1}{4}$	$\frac{1}{8}$	$-\frac{1}{16}$	0
$P11$	$a\ a\ a\ a\ a\ a$	$\frac{1}{6}$	$\frac{1}{12}$	$\frac{1}{12}$	0
$P12$	$a\ a\ a\ a\ a\ -a$	$\frac{1}{6}$	$\frac{1}{12}$	$-\frac{1}{36}$	0

parameter components can change widely during the transition without costing any energy, large fluctuations will be present at such a transition point. Moreover, degeneracies along the line must be lifted by including small sixth-degree terms in the free-energy expansion. These considerations implicate that the transition is actually of first order. A detailed analysis will be published elsewhere.

V. IMAGES $L4$, $L6$, AND $L8$

Consider the images $L4$, $L6$, and $L8$. The free energy to the fourth degree is written

$$G=\frac{a}{2}I_2+\tfrac{1}{4}(A_0I_2^2+A_1I_1^{(4)}+A_2I_2^{(4)}+A_3I_3^{(4)})$$
$$\equiv\frac{a}{2}\eta^2+\tfrac{1}{4}\eta^4(A_0+A_1\lambda_1+A_2\lambda_2+A_3\lambda_3)\ . \quad (4)$$

The directional minimum of the quartic potential is given by

$$\eta_0^2=-\frac{a}{A_0+A_1\lambda_1+A_2\lambda_2+A_3\lambda_3}\ , \quad (5)$$

TABLE V. Stable phases in each region of the (A_1,A_2) space: Images $L1$, $L2$, $L3$, and $L5$.

Region	Stable phase	
$A_1>0,\ A_2>0$	$(P6,P7)$:	$2A_1-A_2<0$
	$(P11,P12)$:	$2A_1-A_2>0$
$A_1>0,\ A_2<0$	$P2$:	$2A_1+A_2<0$
	$(P11,P12)$:	$2A_1+A_2>0$
$A_1<0,\ A_2>0$	$P1$:	everywhere
$A_1<0,\ A_2<0$	$P1$:	$2A_1-A_2<0$
	$P2$:	$2A_1-A_2>0$

$$G_0=-\frac{1}{4}\frac{a^2}{A_0+A_1\lambda_1+A_2\lambda_2+A_3\lambda_3}\ . \quad (6)$$

The projected "orbit space" $(\lambda_1,\lambda_2,\lambda_3)$ is too complicated. Thus we project it further:

$$A_2\lambda_2+A_3\lambda_3\equiv A[\cos(\theta)\lambda_2+\sin(\theta)\lambda_3]\equiv A\lambda'(\theta)\ , \quad (7)$$

$$G_0=-\frac{1}{4}\frac{a^2}{A_0+A_1\lambda_1+A\lambda'(\theta)}\ . \quad (8)$$

The projected "orbit spaces" $(\lambda_1,\lambda'(\theta))$ at several angles θ are depicted in Fig. 2. At a fixed angle θ we can find the absolute minimum in the same way as we did in Sec. IV. Let us find stable phases in various regions of (A_1,A,θ) space.

Region I: $A<0$, $A_1>0$. The contour of the directional minima is a straight line with positive slope (λ_1 increases as λ' increases). The minimum value increases as the contour moves in the upper-left direction. The possible phases at different angles θ are

(i) $0°<\theta<63.4°$ $(=\tan^{-1}2)$: $P2,P11$,

(ii) $63.4°<\theta<135°$: $P11$,

(iii) $135°<\theta<180°$: $P11,(P6,P7)$.

Region II: $A<0$, $A_1<0$. The contour has a negative slope and moves in the lower-left direction:

(i) $0°<\theta<63.4°$: $P1,P2$,

(ii) $63.4°<\theta<76.0°$ $(=\tan^{-1}4)$: $P1,P2,P11$,

(iii) $76.0°<\theta<135°$: $P1,P11$,

(iv) $135°<\theta<180°$: $P1$.

Region III: $A>0$, $A_1<0$. The contour has a positive slope and moves in the lower-right direction:

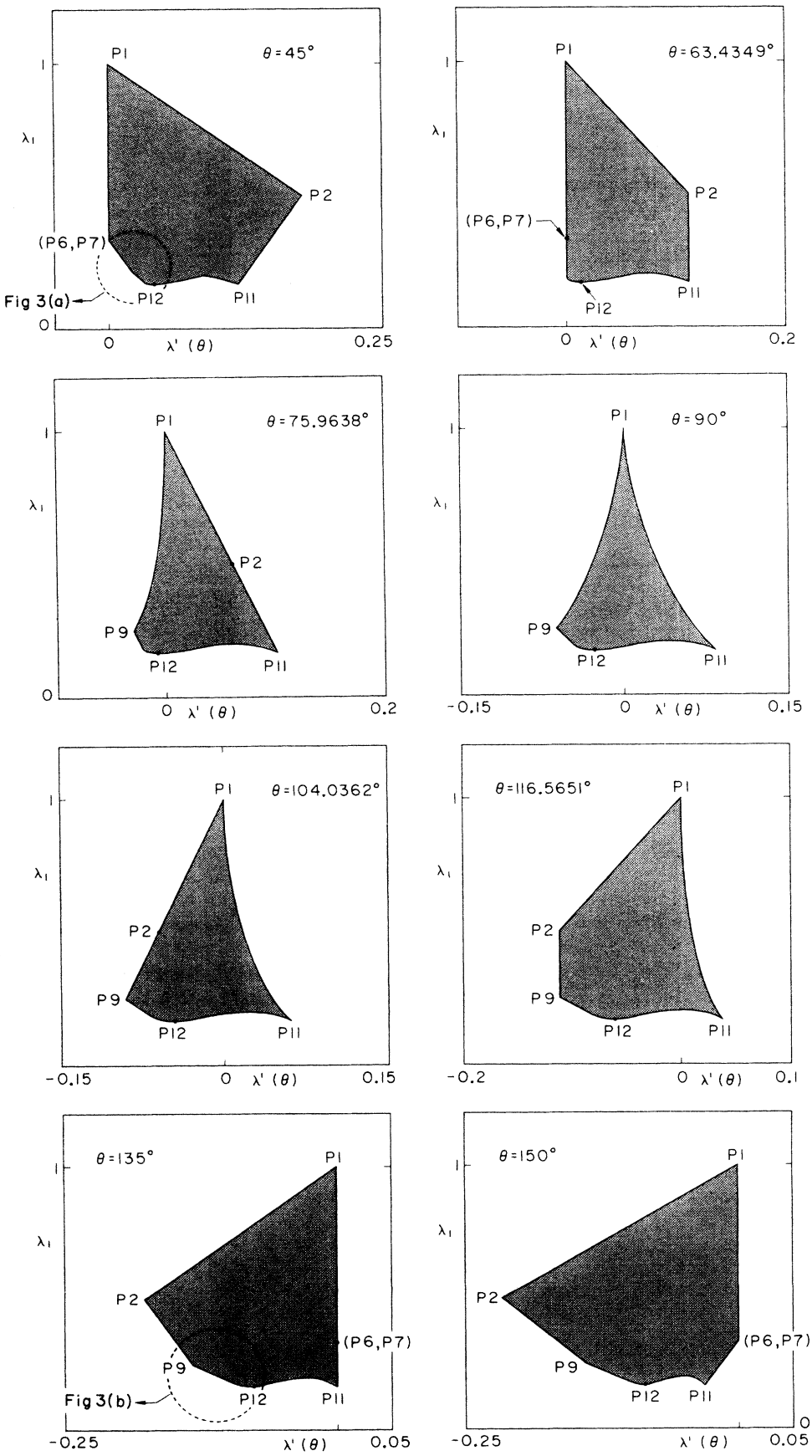

FIG. 2. The "orbit space" $(\lambda_1, \lambda'(\theta))$ of images $L4$, $L6$, and $L8$ at several angles θ.

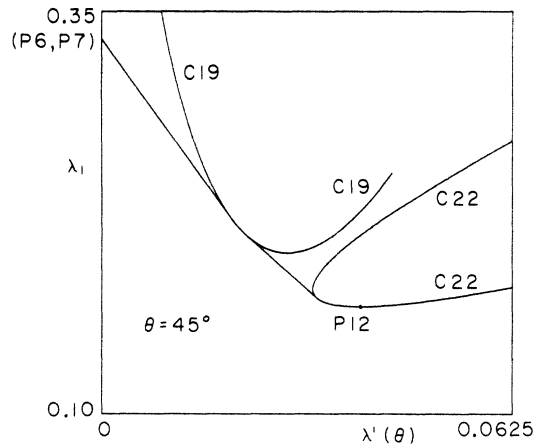

(a)

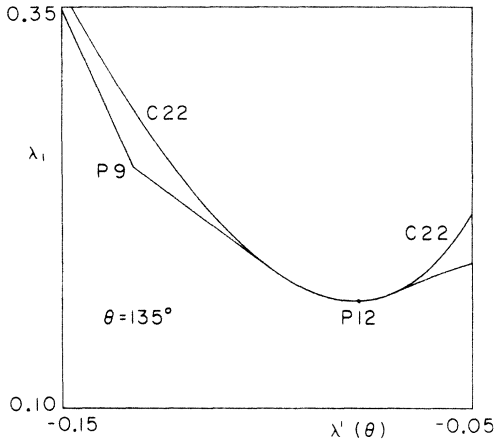

(b)

FIG. 3. The enlarged diagrams of the lower-left corner of the "orbit space" $(\lambda_1, \lambda'(\theta))$ at $\theta=45°, 135°$.

(i) $0°<\theta<63.4°$: $P1$,

(ii) $63.4°<\theta<104.0°$ $[=\tan^{-1}(-4)]$: $P1,P9$,

(iii) $104.0°<\theta<116.6°$ $[=\tan^{-1}(-2)]$: $P1,P9,P2$,

(iv) $116.6°<\theta<180°$: $P1,P2$.

Region IV: $A>0$, $A_1>0$. The contour has a negative slope and moves in the upper-right direction. The lower-left portion of the "orbit-space" boundary is convex and consists of many different orbits (see Fig. 3):

(i) $0°<\theta<63.4°$: $(P6,P7), C19, C22$,

(ii) $63.4°<\theta<116.6°$: $P9, C22$,

(iii) $116.6°<\theta<180°$: $P2,P9,C22$.

The stable phases in regions I—III are easily obtained by comparing the directional minimum values of the Landau potential in competing directions. For example, let us consider region II, case (ii):

$A<0$, $A_1<0$, $63.4°<\theta<76.0°$.

$P1$ is stable in the subregion $G_0(P1)<G_0(P2)$, i.e.,

$$\tfrac{1}{2}A_1-\tfrac{1}{4}A_2<0 .$$

$P2$ is stable in the subregion $G_0(P2)<G_0(P1)$ and $G_0(P2)<G_0(P11)$, i.e.,

$$\tfrac{1}{2}A_1-\tfrac{1}{4}A_2>0 \text{ and } \tfrac{1}{3}A_1+\tfrac{1}{6}A_2-\tfrac{1}{12}A_3<0 .$$

$P3$ is stable in the subregion $G_0(P11)<G_0(P2)$, i.e.,

$$\tfrac{1}{3}A_1+\tfrac{1}{6}A_2-\tfrac{1}{12}A_3>0 .$$

In part (a) of Table VI we tabulate the stable phases in the corresponding subregions of (A_1,A_2,A_3) space.

When a phase of subduction frequency greater than one is eligible, it is no longer possible to find the minimum in an analytic form. This is the case in region IV. We will illustrate how to find the absolute minimum at $\theta=45°$ and 135°. The stable phases at all angles θ are listed in part (a) Table VI. Let us parametrize the slope of the contour by an angle ϕ: $\tan\phi\equiv A/A_1$.

Consider the case, $\theta=45°$. For $\phi>80.0°\equiv\phi_U$, the contour is close to the vertical line and the point $(P6,P7)$ yields the absolute minimum. For $\phi_L\equiv 74.6°<\phi<80.0°$, the protrudent portion [Fig. 3(a)] of the curve $C19$ yields the absolute minimum. For $\phi<74.6°$ the boundary portion of the curve $C22$ yields the absolute minimum. As θ deviates towards 63.4° or 0°, the phase volume $\Delta\phi=\phi_U-\phi_L$ for $C19$ diminishes. The upper and lower limits at other angles θ, $\phi_U(\theta)$ and $\phi_L(\theta)$, are tabulated in part (b) of Table VI. Here we have established that $C19$ and $C22$ yield the absolute minimum in region IV, case (i): $\phi_L<\phi<\phi_U$ and $\phi<\phi_L$, respectively. Since a point on a curve is specified by a single parameter, one can get the minimum (located on the curves $C19$ and $C22$) as accurately as the computer allows.

Consider the case $\theta=135°$. At large angles ϕ, i.e., when $4A_1+2A_2+A_3<0$, $P2$ gives the absolute minimum. In the region $4A_1+2A_2+A_3>0$ and $\phi>62°\equiv\phi_C$, $P9$ gives the minimum. Finally, in the region $\phi<\phi_C$, $C22$ yields the minimum. The limiting angle $\phi_C(\theta)$ is tabulated in part (c) of Table VI.

Here again the degeneracy between $P6$ and $P7$ can be lifted by a small sixth-degree term $I_3^{(6)}$. The orbit $P12$ is a special point on the orbit $C22$ and the corresponding phase can be realized at an isolated point in the P-T plane. However, a slight deviation from the point can easily move the absolute minimum to either $P11$ or $C22$.

A. Images $L4$ and $L6$

$L4$ and $L6$ have the identical integrity basis up to the sixth degree. They begin to be different at the seventh degree. $L6$ has a seventh degree invariant, whereas $L4$ does not.

The two phases $C19$ and $C22$ in the region $A>0$ and $A_1>0$ comprise counterexamples to the Michel-Radicati conjecture.[22] In previous work[24] the phase $C22$ of a submaximal isotropy subgroup was found to be eligible. However, the phase $C19$ was not found by any previous

TABLE VI. (a) Stable phases in each region of (A_1, A_2, A_3) space: Images $L4$, $L6$, and $L8$. The angle ϕ is defined as $\tan\phi \equiv A/A_1$, where $A^2 \equiv A_2^2 + A_3^2$ and $\tan\theta \equiv A_3/A_2$ [see Eq. (7)]. (b) Limiting angles $\phi_U(\theta)$ and $\phi_L(\theta)$ to be used in the region $A > 0$, $A_1 > 0$ and $0 < \theta < 63.43°$. (c) Limiting angle $\phi_C(\theta)$ to be used in the region $A > 0$, $A_1 > 0$ and $\theta > 63.43°$.

(a)

Region		Stable phase	
$A < 0$, $A_1 > 0$	$0° < \theta < 63.43°$	$P2$:	$4A_1 + 2A_2 - A_3 < 0$
		$P11$:	$4A_1 + 2A_2 - A_3 > 0$
	$63.43° < \theta < 135°$	$P11$:	everywhere
	$135° < \theta < 180°$	$(P6, P7)$:	$2A_1 - A_2 - A_3 < 0$
		$P11$:	$2A_1 - A_2 - A_3 > 0$
$A < 0$, $A_1 < 0$	$0° < \theta < 63.43°$	$P1$:	$2A_1 - A_2 < 0$
		$P2$:	$2A_1 - A_2 > 0$
	$63.43° < \theta < 75.96°$	$P1$:	$2A_1 - A_2 < 0$
		$P2$:	$4A_1 + 2A_2 - A_3 < 0$ and $2A_1 - A_2 > 0$
		$P11$:	$4A_1 + 2A_2 - A_3 > 0$
	$75.96° < \theta < 135°$	$P1$:	$10A_1 - A_2 - A_3 < 0$
		$P11$:	$10A_1 - A_2 - A_3 > 0$
	$135° < \theta < 180°$	$P1$:	everywhere
$A > 0$, $A_1 < 0$	$0° < \theta < 63.43°$	$P1$:	everywhere
	$63.43° < \theta < 104.04°$	$P1$:	$12A_1 - 2A_2 + A_3 < 0$
		$P9$:	$12A_1 - 2A_2 + A_3 > 0$
	$104.04° < \theta < 116.57°$	$P1$:	$2A_1 - A_2 < 0$
		$P2$:	$4A_1 + 2A_2 + A_3 < 0$ and $2A_1 - A_2 > 0$
	$116.57° < \theta < 180°$	$P9$:	$4A_1 + 2A_2 + A_3 > 0$
		$P1$:	$2A_1 - A_2 < 0$
		$P2$:	$2A_1 - A_2 > 0$
$A > 0$, $A_1 > 0$	$0° < \theta < 63.43°$	$(P6, P7)$:	$\phi > \phi_U$
		$C19$:	$\phi_L < \phi < \phi_U$
		$C22$:	$\phi < \phi_L$
	$63.43° < \theta < 116.57°$	$P9$:	$\phi > \phi_C$
		$C22$:	$\phi < \phi_C$
	$116.57° < \theta < 180°$	$P2$:	$4A_1 + 2A_2 + A_3 < 0$
		$P9$:	$4A_1 + 2A_2 + A_3 > 0$ and $\phi > \phi_C$
		$C22$:	$\phi < \phi_C$

(b)

θ (deg)	$\phi_U(\theta)$	$\phi_L(\theta)$
5	64.5311	63.5651
10	65.8203	63.9541
15	67.3025	64.6029
20	68.9762	65.5165
25	70.8377	66.7038
30	72.8805	68.1785
35	75.0945	69.9597
40	77.4656	72.0754
45	79.9750	74.5680
50	82.5997	77.5098
55	85.3122	81.0450
60	88.0817	85.5545

(c)

θ (deg)	$\phi_C(\theta)$	θ (deg)	$\phi_C(\theta)$
65	89.1253	125	63.8224
70	86.3430	130	62.8465
75	83.6054	135	62.0616
80	80.9445	140	61.4662
85	78.3890	145	61.0587
90	75.9638	150	60.8379
95	73.6891	155	60.8032
100	71.5809	160	60.9543
105	69.6506	165	61.2919
110	69.9061	170	61.8169
115	66.3521	175	62.5307
120	64.9906	180	63.4349

authors. Note that $C19$ is a special curve on the two-dimensional orbit $S12$ in the case of $L6$.

B. Image $L8$

$P9$ (see image $L4$ in Table IV for direction) is a special point on the orbit $C12$ of a submaximal isotropy subgroup in the case of $L8$ (whereas its isotropy subgroup was maximal in the case of $L4$ and $L6$). Since the symmetry group of the quartic potential is the supergroup of the physical symmetry, the Ascher conjecture is violated. $C19$ is a special curve on the four-dimensional orbit $4D4$. $C22$ is a special curve on the two-dimensional orbit $S16$. These two phases form counterexamples to the Michel-Radicati conjecture.

Note that the symmetry level of $C19$ is lowered by one as we go from $L4$ to $L6$, and those of $C19$ and $C22$ are lowered by three and one, respectively, as we descend from $L4$ to $L8$ (see Fig. 2 of Ref. 31). This is due to the lack of available high-level isotropy subgroups because $L8$ is small. The violation of the Ascher conjecture occurs for the same reason. However, the violation of the Michel-Radicati conjecture has to do more with the orbit-space geometry than with the difference in sizes of the physical and quartic potential symmetries. If the violation occurs, it occurs already with the largest symmetry group of the quartic potential. Here the violation is due to the invariant $I_3^{(4)}$, which is somewhat less symmetric than the others. Since $I_3^{(4)}$ also appears in the three remaining images ($L7$, $L9$, and $L10$ in the notation of Tolédano and Tolédano) and none of the maximal isotropy subgroups corresponds to $C19$ or $C22$, the Michel-Radicati conjecture is violated in all these six-dimensional images.

TABLE VII. (a) Stable phases in each region of (A_1,A_2,A_7) space: Image $L11$. The angle ξ is defined as $\tan\xi\equiv|B/A_1|$, where $B^2\equiv A_2^2+A_7^2$ and $\tan\theta\equiv A_7/A_2$ [see Eq. (10)]. (b) Limiting angles $\xi_L(\theta)$ and $\xi_R(\theta)$ to be used in (a). For $\theta>90°$, the limiting angles are given by $\xi_L(\theta)=\xi_R(\theta-90°)$ and $\xi_R(\theta)=\xi_L(\theta-90°)$.

(a)

Region	Phase	
$B<0$, $A_1>0$	$C1$:	$\xi>\xi_R$
	$C23$:	$\xi<\xi_R$
$B<0$, $A_1<0$	$C1$:	everywhere
$B>0$, $A_1<0$	$C1$:	everywhere
$B>0$, $A_1>0$	$C1$:	$\xi>\xi_L$
	$C23$:	$\xi<\xi_L$

(b)

θ (deg)	$\xi_L(\theta)$	$\xi_R(\theta)$
5	89.8912	63.4351
10	89.5680	63.4376
15	89.0400	63.4478
20	88.3220	63.4743
25	87.4330	63.5273
30	86.3950	63.6179
35	85.2316	63.7570
40	83.9673	63.9551
45	82.6264	64.2212
50	81.2326	64.5633
55	79.8085	64.9880
60	78.3753	65.5003
65	76.9524	66.1042
70	75.5572	66.8018
75	74.2050	67.5943
80	72.9091	68.4812
85	71.6807	69.4605
90	70.5288	70.5288

VI. IMAGE $L11$

This is the image that previous authors[31] missed. The free energy to the fourth degree is written:

$$G=\frac{a}{2}I_2+\tfrac{1}{4}(A_0I_2^2+A_1I_1^{(4)}+A_2I_2^{(4)}+A_7I_7^{(4)})$$
$$\equiv\frac{a}{2}\eta^2+\tfrac{1}{4}\eta^4(A_0+A_1\lambda_1+A_2\lambda_2+A_7\lambda_7)\,. \quad (9)$$

Here again we project the "orbit space" $(\lambda_1,\lambda_2,\lambda_7)$ to

$$A_2\lambda_2+A_7\lambda_7\equiv B[\cos(\theta)\lambda_2+\sin(\theta)\lambda_7]\equiv B\lambda''(\theta)\,. \quad (10)$$

The projected "orbit spaces" $(\lambda_1,\lambda''(\theta))$ at several angles θ are depicted in Fig. 4. The "orbit space" at an angle θ greater than 90° is the mirror image of that at $\theta-90°$, reflected with respect to the vertical axis $\lambda''=0$. The convex portions of the "orbit-space" boundary correspond to $C1$ and $C23$ of maximal isotropy subgroups.

The absolute minimum of the free energy is found in the same way as in Sec. V. Let us define an angle ξ: $\tan\xi\equiv|B/A_1|$. Let us consider a typical region $B>0$, $A_1>0$ and $\theta=45°$. For $\xi>82.6°\equiv\xi_L$ the contour is close to the vertical line. Thus $C1$ gives the absolute minimum. For $\xi<\xi_L$ it is $C23$ that yields the minimum. $\xi_L(\theta)$ is tabulated in part (b) of Table VII. $\xi_R(\theta)$ is the limiting angle for the region $B<0$, $A_1>0$. The stable phases in various regions are listed in part (a) of Table VII.

VII. SUMMARY AND CONCLUSION

For a class of six-dimensional images we have made lists of stable phases that can be realized in continuous phase transitions. We have presented the phase structure (the phase diagram) in each case. With the forthcoming table of isotropy subgroups (Stokes and Hatch)[20(b)] experimentalists can rapidly compare observed space-group changes against our lists or use our lists in a predictive manner.

Also the above considerations of solid systems with six-component order parameters have exhibited some rather interesting features. In all cases the fourth-degree potential does not distinguish two phases $P6$ and $P7$, which makes it necessary to include a small perturbative sixth-degree term $I_3^{(6)}$. The Landau potential for images $L1$, $L2$, and $L3$ allows stable phases, preserving maximal symmetries. For space-group representations with images $L5$ and $L8$, observation of phases ($P11$,$P12$) and $P9$ will confirm the violation of the Ascher conjecture at work in physical solids. It will be interesting to see experimentally

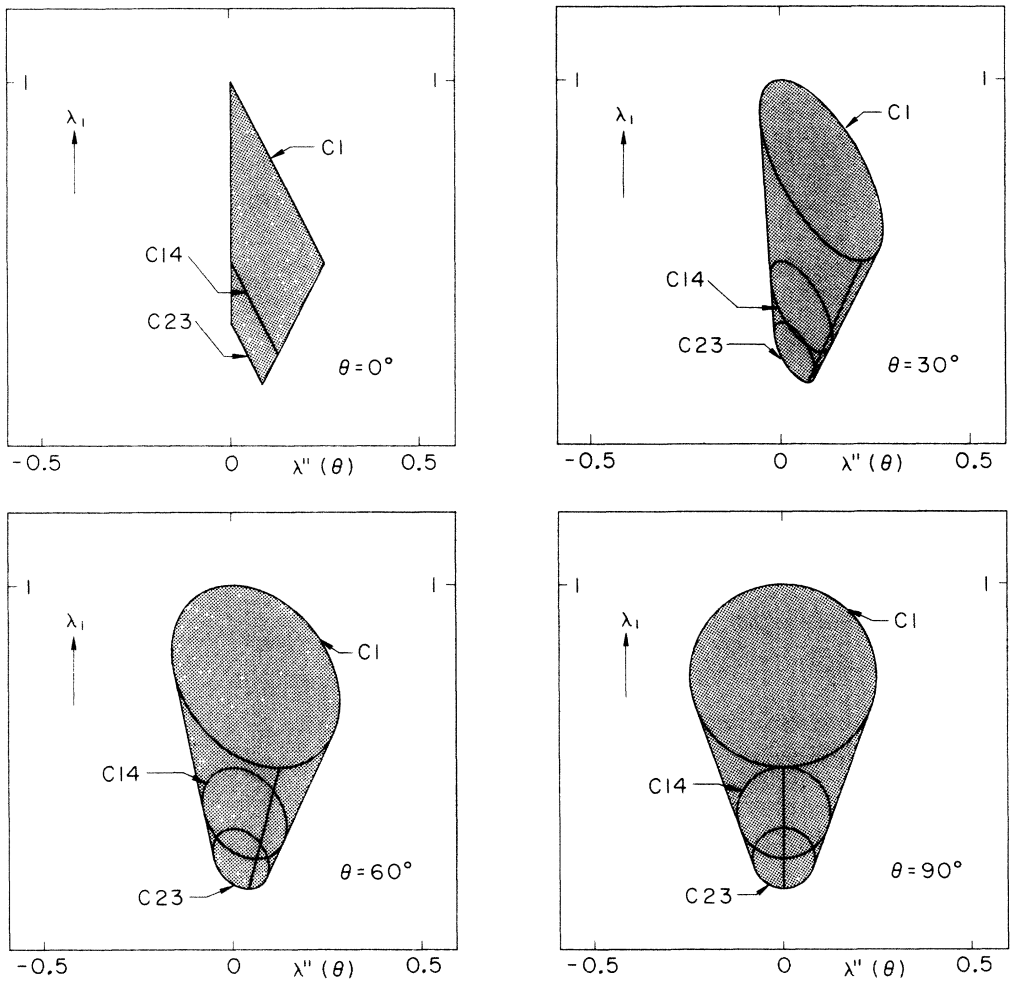

FIG. 4. The "orbit space" $(\lambda_1, \lambda''(\theta))$ of image $L11$ at several angles θ.

TABLE VIII. Isotropy subgroups of orbits $P9$, $C19$, and $C22$ for each space-group representation violating the maximality conjectures. In the case of $L6$, $C19$ belongs to $S12$. In the case of $L8$, $P9$ belongs to $C2$, $C19$ to $4D4$, and $C22$ to $S16$.

Image	Irrep		Space group		$P9$		$C19$		$C22$
$L4$	X_3	O_h^4	($Pn3m$; No. 224)	D_{2d}^3	($P\bar{4}2_1m$; No. 113)	C_{2v}^{12}	($Cmc2_1$; No. 36)	D_4^4	($P4_12_12$; No. 92)
	X_4	O_h^4	($Pn3m$; No. 224)	D_{2d}^3	($P\bar{4}2_1m$; No. 113)	C_{2v}^{12}	($Cmc2_1$; No. 36)	D_4^8	($P4_32_12$; No. 96)
	N_1^-	O_h^9	($Im3m$; No. 229)	D_{4h}^{20}	($I4_1/acd$; No. 142)	C_{2v}^{19}	($Fdd2$; No. 43)	D_{2d}^{10}	($I\bar{4}c2$; No. 120)
	N_2^-	O_h^9	($Im3m$; No. 229)	D_{4h}^{20}	($I4_1/acd$; No. 142)	C_{2v}^{19}	($Fdd2$; No. 43)	C_{4v}^{10}	($I4cm$; No. 108)
	N_3^-	O_h^9	($Im3m$; No. 229)	D_{4h}^{17}	($I4/mmm$; No. 139)	C_{2v}^{18}	($Fmm2$; No. 42)	D_{2d}^9	($I\bar{4}m2$; No. 119)
	N_4^-	O_h^9	($Im3m$; No. 229)	D_{4h}^{17}	($I4/mmm$; No. 139)	C_{2v}^{18}	($Fmm2$; No. 42)	C_{4v}^{11}	($I4_1md$; No. 109)
$L6$	N_2	O^5	($I432$; No. 211)	D_4^{10}	($I4_122$; No. 98)	C_2^3	($B2$; No. 5)	C_4^5	($I4$; No. 79)
	N_4	O^5	($I432$; No. 211)	D_4^9	($I422$; No. 97)	C_2^3	($B2$; No. 5)	C_4^6	($I4_1$; No. 80)
	N_2	T_d^3	($I\bar{4}3m$; No. 217)	D_{2d}^{12}	($I\bar{4}2d$; No. 122)	C_{1h}^4	(Bb; No. 9)	S_4^2	($I\bar{4}$; No. 82)
	N_3	T_d^3	($I\bar{4}3m$; No. 217)	D_{2d}^{11}	($I\bar{4}2m$; No. 121)	C_{1h}^3	(Bm; No. 8)	S_4^2	($I\bar{4}$; No. 82)
	M_2	O_h^2	($Pn3n$; No. 222)	D_{2d}^{12}	($I\bar{4}2d$; No. 122)	C_{1h}^4	(Bb; No. 9)	C_4^5	($I4$; No. 79)
	M_4	O_h^4	($Pn3m$; No. 224)	D_{2d}^{11}	($I\bar{4}2m$; No. 121)	C_{1h}^3	(Bm; No. 8)	C_4^6	($I4_1$; No. 80)
	X_4	O_h^7	($Fd3m$; No. 227)	D_{2d}^3	($P\bar{4}2_1m$; No. 113)	C_{1h}^3	(Bm; No. 8)	C_4^2	($P4_1$; No. 76)

TABLE VIII. (*Continued*).

Image	Irrep		Space group	$P9$		$C19$		$C22$	
$L6$	X_4	O_h^8	($Fd3c$; No. 228)	D_{2d}^4	($P\bar{4}2_1c$; No. 114)	C_{1h}^4	(Bb; No. 9)	C_{4v}^2	($P4_1$; No. 76)
	N_2^+	O_h^9	($Im3m$; No. 229)	D_{4h}^{19}	($I4_1/amd$; No. 141)	C_{2h}^6	($B2/b$; No. 15)	C_{4h}^5	($I4/m$; No. 87)
	N_4^+	O_h^9	($Im3m$; No. 229)	D_{4h}^{18}	($I4/mcm$; No. 140)	C_{2h}^3	($B2/m$; No. 12)	C_{4h}^6	($I4_1/a$; No. 88)
$L8$	N_1^-	T_h^5	($Im3$; No. 204)	D_{2h}^{27}	($Ibca$; No. 73)	C_{1h}^4	(Bb; No. 9)	C_{2v}^{21}	($Iba2$; No. 45)
	N_2^-	T_h^5	($Im3$; No. 204)	D_{2h}^{25}	($Immm$; No. 71)	C_{1h}^3	(Bm; No. 8)	C_{2v}^{20}	($Imm2$; No. 44)

phases $C19$ and $C22$ of nonmaximal symmetries in a physical system whose order parameter transforms as a representation whose image is $L4$, $L6$, or $L8$, and to theoretically explain microscopic mechanisms for the violation of the Michel-Radicati conjecture. The image $L8$ is particularly interesting because both conjectures are violated in a single physical system. We indicate in Table VIII the space-group changes corresponding to $C19$ and $C22$ in images $L4$, $L6$, and $L8$. Further lists of continuous phase transitions corresponding to order parameters of arbitrary components will be published in near future.

ACKNOWLEDGMENTS

We would like to thank Professor L. Michel for enlightening discussions and A. Giambattista for checking the invariants in Table II.

[1]L. D. Landau, Phys. Z. Sowjetunion **11**, 26 (1937); **11**, 545 (1937); L. D. Landau and E. M. Lifshitz, *Statistical Physics* (Addison-Wesley, Reading, Mass., 1958).

[2]G. Ya. Lyubarskii, *The Application of Group Theory in Physics* (Pergamon, New York, 1960), Chap. VII.

[3]E. M. Lifshitz, J. Phys. (Moscow) **6**, 61 (1942).

[4]J. L. Birman, Phys. Rev. Lett. **17**, 1216 (1966).

[5]F. E. Goldrich and J. L. Birman, Phys. Rev. **167**, 528 (1968).

[6]M. V. Jaric and J. L. Birman, Phys. Rev. B **16**, 2564 (1977); M. V. Jaric, Ph.D. thesis, City University of New York, 1977 (unpublished); M. V. Jaric, Phys. Rev. B **23**, 3460 (1981).

[7]D. M. Hatch, Phys. Rev. B **23**, 2346 (1981).

[8]E. B. Vinberg, Yu. M. Gufan, V. P. Sakhnenko, and Yu. I. Sirotin, Kristallografiya **17**, 336 (1972) [Sov. Phys.—Crystallogr. **19**, 10 (1974)].

[9]J. S. Kim, Nucl. Phys. **196B**, 285 (1982); **197B**, 174 (1982); S. Frautschi and J. S. Kim, *ibid.* **196B**, 301 (1982); J. S. Kim, J. Math. Phys. **25**, 1694 (1984); Phys. Rev. B **31**, 1433 (1985).

[10]L. Michel, in *Lectures in Theoretical Physics,* edited by K. T. Mahanthappa *et al.* (Gordon and Breach, New York, 1969), Vol. XI-A, p. 263.

[11]G. E. Bredon, *Introduction to Compact Transformation Groups* (Academic, New York, 1972).

[12]There are several review articles for physicists; see L. Michel, in *Regards sur la Physique Contemporaine* (CNRS, Paris, 1980), pp. 157–203; L. O'Raifeartaigh, Rep. Prog. Phys. **42**, 159 (1979); M. Abud and G. Sartori, Ann. Phys. (N.Y.) **150**, 307 (1983).

[13]S. Deonarine and J. L. Birman, Phys. Rev. B **27**, 4261 (1983).

[14]A. P. Cracknell, B. L. Davis, S. C. Miller, and W. F. Love, *Kronecker Product Tables* (IFI/Plenum, New York, 1979).

[15]O. V. Kovalev, *Irreducible Representations of Space Groups* (Gordon and Breach, New York, 1965); J. Zak, A. Cacher, H. Glück, and Y. Gur, *The Irreducible Representations of Space Groups* (Benjamin, New York, 1969).

[16]M. V. Jaric, J. Math. Phys. **24**, 917 (1983).

[17]D. M. Hatch, in *Group Theoretical Methods in Physics, Trieste, 1983,* Vol. 201 of *Lecture Notes in Physics,* edited by G. Denardo, G. Ghirardi, and T. Weber (Springer, New York, 1984), p. 390.

[18]L. Michel and J. Mozrzymas, in *Group Theoretical Methods in Physics, Tübingen, 1979,* Vol. 79 of *Lecture Notes in Physics,* edited by P. Kramer and A. Rieckers (Springer, Berlin, 1978), p. 447; M. V. Jaric, L. Michel, and R. T. Sharp, J. Phys. (Paris) **45**, 1 (1984).

[19]J. R. Zielinski, W. J. Cieslwicz, and W. Marsec, J. Phys. C **12**, 4721 (1979); **13**, 3835 (1980); J. M. Pérez-Mato, J. L. Mañes, M. J. Tello, and F. J. Zúñiga, *ibid.* **14**, 1121 (1981); M. V. Jaric, Phys. Rev. B **25**, 2015 (1982); M. Sutton and R. L. Armstrong, *ibid.* **25**, 1813 (1982); **27**, 1937 (1983); M. H. Ben Ghozlen and Y. Mlik, J. Phys. C **16**, 4365 (1983); H. T. Stokes and D. M. Hatch, Phys. Rev. B **30**, 3845 (1984).

[20](a) H. T. Stokes and D. M. Hatch, Phys. Rev. B **30**, 4962 (1984); D. M. Hatch and H. T. Stokes, *ibid.* **30**, 5156 (1984); (b) unpublished.

[21]E. Ascher, J. Phys. C **10**, 1365 (1977).

[22]L. Michel and L. A. Radicati, in *Evolution of Particle Physics,* edited by M. Conversi (Academic, New York, 1970), p. 191.

[23]J.-C. Tolédano and P. Tolédano, J. Phys. (Paris) **41**, 189 (1980).

[24]D. Mukamel and M. V. Jaric, Phys. Rev. B **29**, 1465 (1984).

[25]A good review is given in P. Tolédano and G. Pascoli, in *Symmetries and Broken Symmetries in Condensed Matter Physics,* edited by N. Boccara (IDSET, Paris, 1981), p. 291.

[26]A. F. Devonshire, Philos. Mag. **40**, 1040 (1949); **42**, 1065 (1951).

[27]A. P. Levanyuk and D. Sannikov, Zh. Eksp. Teor. Fiz. **60**, 1109 (1971) [Sov. Phys.—JETP **33**, 600 (1971)]; K. S. Aleksandrov and V. I. Zinenko, Fiz. Tverd. Tela. (Leningrad) **12**, 2092 (1970) [Sov. Phys.—Solid State **12**, 1662 (1971)].

[28]J. S. Kim, Nucl. Phys. **207B**, 374 (1982); S. Galam and J. L. Birman, Phys. Rev. Lett. **51**, 1066 (1983).

[29]D. M. Hatch and H. T. Stokes, Phys. Rev. B **31**, 4350 (1985).
[30]Yu. M. Gufan and V. P. Sakhnenko, Zh. Eksp. Teor. Fiz. **63**, 1909 (1972) [Sov. Phys.—JETP **36**, 1009 (1973)].
[31]J.-C. Tolédano and P. Tolédano, Phys. Rev. B **21**, 1139 (1980).
[32]P. Tolédano and E. Meimarakis, Ferroelectrics **55**, 329 (1984).
[33]T. Hahn, *International Tables for Crystallography* (Reidel, Dordrecht, 1983), Vol. A.
[34]D. M. Hatch and H. T. Stokes, Phys. Rev. B **31**, 2908 (1985).
[35]J. S. Kim, D. M. Hatch, and H. T. Stokes, in Proceedings of the VIth International Meeting on Ferroelectricity, Kobe, Japan, 1985 [Jpn. J. Appl. Phys. **24**, Suppl. 3, 471 (1985)].

[36]The space (λ_1,λ_2) is a projection of the space $(\lambda_1,\lambda_2,\ldots,\lambda_{l-1})$, which is, in turn, the cross section of the orbit space $(I_2,\ \lambda_1,\lambda_2,\ldots,\lambda_{l-1})$ at $I_2=1$. A point in the space $(\lambda_1,\lambda_2,\ldots,\lambda_{l-1})$ represents a stratum (Ref. 12) which is a collection of orbits having the same isotropy subgroup (up to conjugation). Thus the space (λ_1,λ_2) is a projected stratum space. In view of the fact that the difference between orbit and stratum is minor, one of us (J.S.K.) (Ref. 9) used a temporary term "orbit space" to designate the space (λ_1,λ_2). To be consistent, we will keep using the term "orbit space."

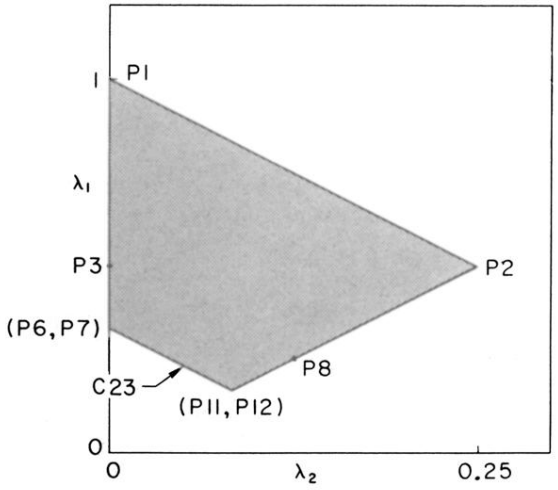

FIG. 1. The "orbit space" (λ_1,λ_2) of images *L*1, *L*2, *L*3, and *L*5

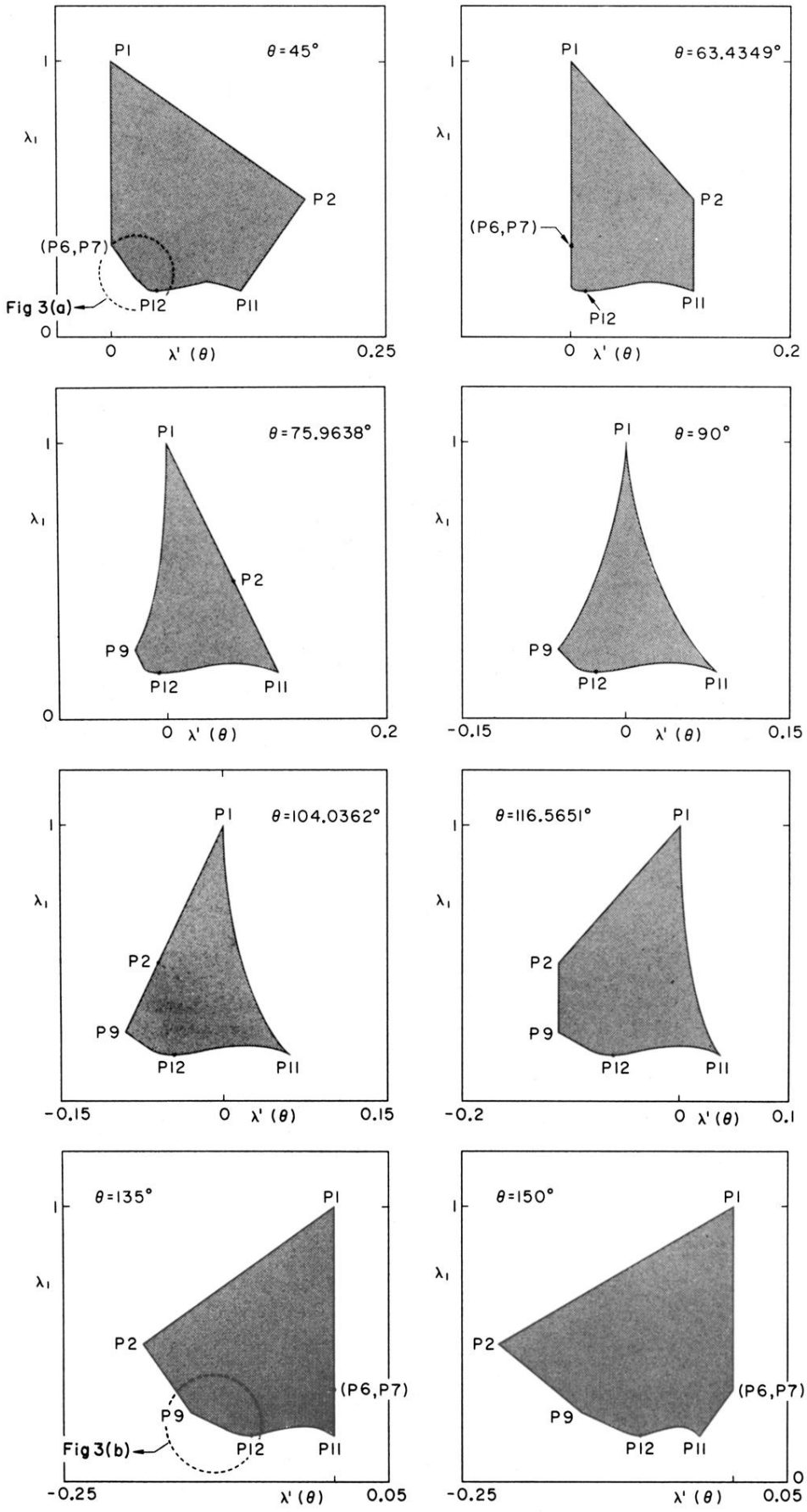

FIG. 2. The "orbit space" $(\lambda_1, \lambda'(\theta))$ of images $L4$, $L6$, and $L8$ at several angles θ.

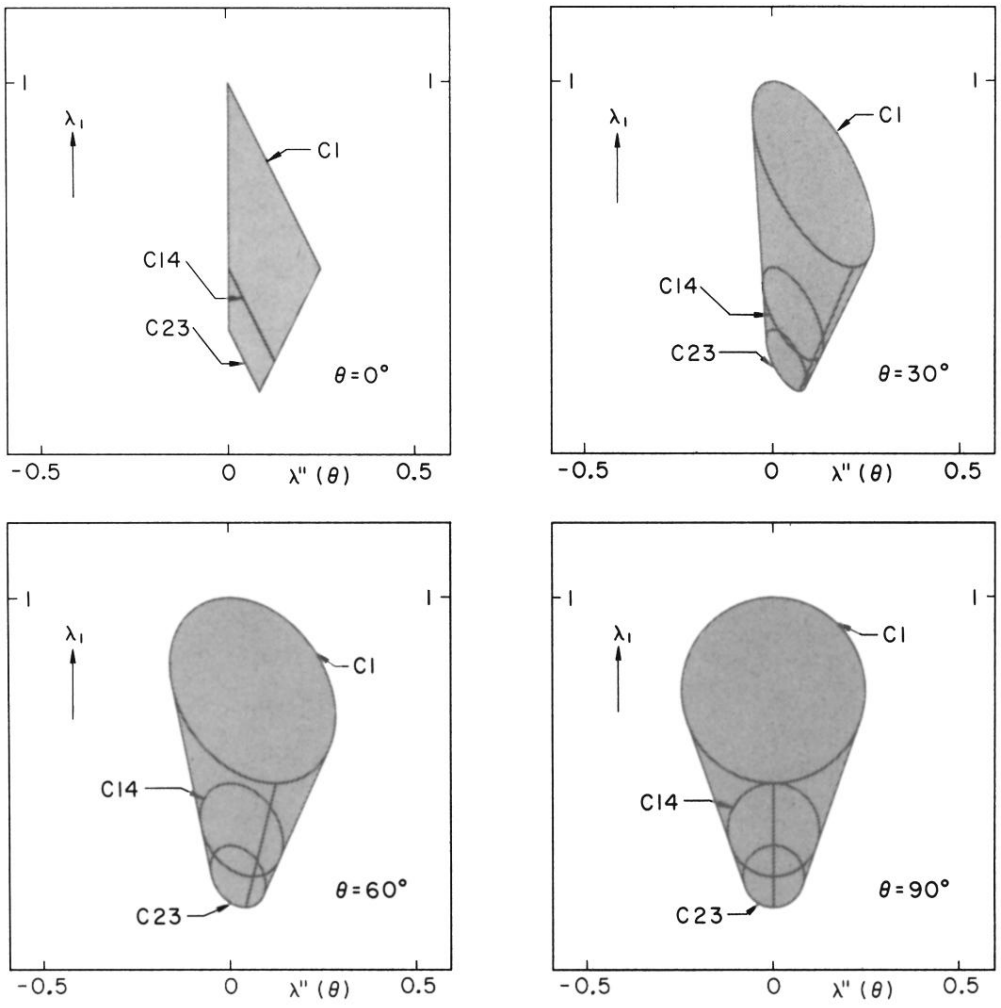

FIG. 4. The "orbit space" $(\lambda_1, \lambda''(\theta))$ of image $L11$ at several angles θ.